Environmental and Experimental Botany 69 (2010) 24–31

Contents lists available at ScienceDirect

Environmental and Experimental Botany

journal homepage: www.elsevier.com/locate/envexpbot

Mapping of nickel in root cross-sections of the hyperaccumulator plant *Berkheya coddii* using laser ablation ICP-MS

Ahmad B. Moradi[a,*], Siegfried Swoboda[b], Brett Robinson[a], Thomas Prohaska[b], Anders Kaestner[c], Sascha E. Oswald[d], Walter W. Wenzel[e], Rainer Schulin[a]

[a] Soil Protection group, Institute of Terrestrial Ecosystems, Dept. of Environmental Science, ETH Zürich, Switzerland
[b] Dept. of Chemistry, University Natural Resources & Applied Life Science, Vienna, Austria
[c] Paul Scherrer Institute, Villigen, Switzerland
[d] Helmholtz Centre for Environmental Research -UFZ, Leipzig, Germany
[e] Dept. of Forest & Soil Science, University Natural Resources & Applied Life Science, Vienna, Austria

ARTICLE INFO

Article history:
Received 7 August 2009
Received in revised form 19 January 2010
Accepted 4 February 2010

Keywords:
Berkheya coddii
Cortex
Dimethylglyoxime
Laser ablation
Nickel
Root cross-section
Stele

ABSTRACT

Quantitative studies of the distribution pattern of metals in plant tissues provide important information on the potential of metal-accumulator plants for remediation and amelioration of contaminated soils. We used laser ablation inductively coupled plasma mass spectrometry (LA-ICP-MS) as well as staining with dimethylglyoxime (DMG) to investigate the distribution pattern of nickel (Ni) in root cross-sections of the Ni-hyperaccumulator plant *Berkheya coddii* Rossler. Plants were grown in rhizoboxes containing soil with 125 mg kg^{-1} Ni. Roots were embedded in resin and cut into sections for LA-ICP-MS analysis. For DMG-staining analysis, fresh root cross-sections were prepared using a microtome. LA-ICP-MS revealed higher Ni concentrations in the cortex (374 ± 66 mg kg^{-1}) than in the stele (210 ± 48 mg kg^{-1}) of the investigated roots. The distribution pattern agreed well with those found by DMG-staining. Higher concentrations of Ni were found in the stele compared to the cortex of roots of the control plants not exposed to elevated soil Ni using both techniques. Our results indicate that an active uptake or ion selection mechanism exists for *B. coddii* in the absence of available Ni in the rhizosphere.

1. Introduction

Hyperaccumulator plants may offer a sustainable treatment option for the remediation of metal-contaminated sites (mining activity, refinery emissions, waste disposal, fossil fuel combustion, and agricultural application of pesticides and biosolids) and also an opportunity to mine naturally metal-rich soils i.e., phytomining of ultramafic soils (Brooks et al., 1998; Angle et al., 2001; Li et al., 2003). *Berkheya coddii* Rossler is a Ni-hyperaccumulator plant that has attracted particular attention because of its high Ni concentration and rapid biomass production. Robinson et al. (1997) reported an annual biomass production of 22 t ha^{-1} and up to 1% (w:w) Ni in the above-ground biomass. The combination of these two traits is rare and makes this plant suitable for the remediation of Ni-contaminated soils by means of phytoextraction. Even though some aspects of metal uptake by hyperaccumulator plants are already known (Kramer et al., 1996; Hall, 2002), these mechanisms might be different among different plants. Unravelling these mechanisms and interactions is necessary in order to improve phytoextraction and phytomining techniques of Ni from contaminated and naturally-rich soils (McNear et al., 2005).

The highest Ni concentration occurs in the shoots of hyperaccumulators. Therefore, shoots and particularly leaf tissue has been the subject of previous investigations (Robinson et al., 2003; Bhatia et al., 2004; Budka et al., 2005; Berazain et al., 2007; de la Fuente et al., 2007; Tappero et al., 2007; Moradi et al., 2009). Proton or nuclear microprobe analyses of *B. coddii* collected from native South African ultramafic soils showed that Ni was concentrated in the mesophyll and epidermis of the leaves (Mesjasz-Przybylowicz et al., 2001). Although roots are the prime site of uptake of metals, the distribution of Ni in root tissues of *B. coddii* has rarely been investigated. Most research regarding Ni hyperaccumulation and uptake has been carried out on Ni hyperaccumulator plants of the family *Brassicaceae* and it is unclear whether other hyperaccumulators have the same uptake mechanism and distribution pattern as the *Brassicaceae* family (Robinson et al., 2003).

Methods currently used for spatial localisation of metals within biological tissues are primarily micro analytical techniques based

Abbreviations: LA-ICP-MS, laser ablation combined with inductively coupled plasma mass spectrometry; DMG, dimethylglyoxime; ICP-OES, inductively coupled plasma optical emission spectrometry; XRF, X-ray fluorescence.

* Corresponding author. Present address: Hydrogeology Department, Helmholtz Centre for Environmental Research - UFZ, Permoserstraße 15, 04318 Leipzig, Germany. Tel.: +49 341 235 1982; fax: +49 341 235 451985.
E-mail address: ahmad.moradi@ufz.de (A.B. Moradi).

0098-8472/$ – see front matter © 2010 Elsevier B.V. All rights reserved.
doi:10.1016/j.envexpbot.2010.02.001

on X-ray emission in response to irradiation with photons or charged particles, including micro-PIXE (micro proton-induced X-ray emission spectroscopy; also known as nuclear microprobe), EDXS (energy dispersive X-ray spectroscopy), Synchrotron X-ray, and Laser-Ablation Inductively-Coupled-Plasma Mass-Spectrometry (LA-ICP-MS) techniques. These methods simultaneously measure and map elemental contents. The choice of suitable analytical method often depends on the investigation level, sampling resolution, detection limit, and accessibility of the technique. Despite the fact that EDXS is a reliable and well-established technique for highly spatially resolved elemental analysis of biological tissues, it has a limited analytical depth and its concentration detection limit (>100–1000 mg kg^{-1}) is insufficient (Ma et al., 2005; Lobinski et al., 2006). Therefore, it has mainly been applied to certain tissues of metal hyperaccumulator plants highly concentrated in metals (Robinson et al., 2003; Broadhurst et al., 2004; Berazain et al., 2007). While micro-PIXE and synchrotron X-ray provide higher analytical sensitivities and penetration than EDXS (Przybylowicz et al., 2001; Lobinski et al., 2006; Fahrni, 2007), their application is limited by accessibility to a proton-beam facility. Laser microprobe mass analysis (LAMMA) showed its potential quite early for analysing thin sections for elemental distribution (Eeckhaoudt et al., 1992). Time of flight SIMS (secondary ion mass spectrometry) was used to study metal distribution between soil, rhizosphere and roots (Martin et al., 2004) and recently, cryo-time-of-flight secondary ion mass spectrometry was applied for element and isotope-specific imaging to monitor transport pathways and processes in the xylem using supplementary sodium and tracers for potassium and rubidium (Metzner et al., 2008). LA-ICP-MS has been suitably applied to determine simultaneously a large number of elements with relatively high detection limits, in the range of μg kg^{-1}, in geological and metallurgical samples (Russo et al., 2002; Hattendorf et al., 2003; Kylander et al., 2007). Recently, LA-ICP-MS was applied successfully to reveal the pattern of copper and zinc in growth zones of cucumber roots (Shi et al., 2009). The spatial resolution of LA-ICP-MS is still insufficient to map the cellular and sub-cellular element distribution, but it benefits from high analytical sensitivity, possibility of isotope ratio measurements, and tracking elemental fluxes by isotope labeling (Pickhardt et al., 2005). Therefore, its application to biological specimens at the tissues-level is emerging (Kindness et al., 2003; Becker et al., 2005; Ulrich et al., 2007; Becker et al., 2008; Kaiser et al., 2008; Shi et al., 2009).

Histochemical staining methods are applied to reveal the elemental distribution for localisation of trace elements within tissues. In particular, dimethylglyoxime (DMG) has been used frequently as histochemical stain for localisation of Ni within tissues of hyperaccumulator plants (Heath et al., 1997; Mizuno et al., 2003; Bhatia et al., 2004; Budka et al., 2005). This method has the potential for qualitative studies of Ni distribution in plant tissues because of its ease of application, low cost of materials and facilities. Although there is usually a risk of artifacts and redistribution of metals inside cells depending on the investigation level and the specific staining procedure used (Bhatia et al., 2004), however, these problems may be alleviated by strict preparation protocols (Gramlich et al., 2007). Such redistribution of metals at the tissue level is less significant than at the sub-cellular level (Budka et al., 2005). Nevertheless, any fixation, sectioning and drying should be performed under low temperature (Budka et al., 2005).

The aim of this study was to map Ni distribution in the root cross-sections of *B. coddii* in order to get a better understanding of its uptake mechanism. We investigated the semi-quantitative spatial distribution of Ni in the root tissues of the hyperaccumulator plant *B. coddii* using LA-ICP-MS. The distribution pattern and the semi-quantitative Ni concentrations determined by means of this technique were compared to the results of the qualitative method, DMG-staining, and bulk analysis by ICP-OES. The advantages and disadvantages of both techniques are discussed in detail.

2. Materials and methods

2.1. Rhizobox experiment and sampling

Seedlings of *B. coddii* were grown for three weeks in perlite before transferred to rhizoboxes with a height of 60 cm, a width of 15 cm and a breadth of 1 cm in the main rooting compartment. Dessureault-Rompre et al. (2006) give a detailed description of these boxes. The narrow breadth facilitated sampling of undisturbed roots for the impregnation in resin. Three rhizoboxes were filled with a sandy soil spiked with 125 mg kg^{-1} Ni, and three with the same unspiked soil as a control. Selected physical and chemical properties of the soil are described in Table 1. We sprayed nickel solution on the soil and stirred the soil well to obtain maximum homogeneity for the spiked soil. The rhizoboxes were irrigated with Hoagland's nutrient solution (Hoagland and Arnon, 1938). The soil water content was maintained near field capacity (25%) by adding 150–200 ml of solution per week. After transplanting, the rhizoboxes were kept in a climate chamber for 8 weeks with a daily light cycle of 16 h light/8 h darkness, constant humidity (75%) and controlled temperature (16/23 °C night/day).

The boxes were dismantled carefully in the 8th week. First, undisturbed soil samples containing roots were taken using samplers with dimensions of 2 cm × 2 cm × 5 cm. The samplers were made of aluminum with sharp edges. They could be inserted into the soil easily and soil samples could be taken with least disturbance. These samples were impregnated in resin and analysed using LA-ICP-MS. We carefully separated the remaining roots from the soil and divided them into groups of the same age and diameter. These samples were used for ICP-OES analysis, DMG-staining as well as LA-ICP-MS analysis (impregnated in resin). The separated root samples were washed carefully with deionised water.

For LA-ICP-MS analysis, the soil samples containing undisturbed roots and as well as the separated root samples were first frozen using liquid nitrogen, freeze-dried and then impregnated under vacuum with an epoxy resin (LR White; London Resin Company Limited, Berkshire, GB). This procedure was performed in order to minimize possible Ni migration during sample preparation. After freeze drying, mobilization can be neglected since no electrolyte solution is available for migration. Heat curing under vacuum was used, with a temperature of 50 °C for a period of 24 h. Subsequently, the samples were cut into sections with height of 15 mm by means of a diamond saw (Accutom-50; Struers, Ballerup, DK). The surfaces were left unpolished to avoid smearing. Resin blanks were prepared and subsequently analysed in the same way as the root cross-sections. We found no traces of Ni or other metals in the blank samples.

For the ICP-OES measurement, the roots were washed with deionised water and dried at 65 °C for 48 h prior to digestion with 15 ml HNO_3 (65%) at 150 °C for 1 h (excluding the heat-up and cool-down time) in Teflon tubes on a heating block (DigiPREP MS, SCP Science, QC, Canada). The digests were checked to be clear and fully digested, then diluted to 20 ml with nanopure water and analysed for Ni, Ca, Mg, and Fe using ICP-OES (Vista-MPX Varian, Australia). We digested and analysed a certified reference material from the Community Bureau of Reference BCR (No. 62, *Olea europaea*) using ICP-OES for quality assurance. Since there was no plant reference material with high enough Ni contents available, we used a standard addition and obtained recoveries in the range of 88–97% for Ni in the certified reference plant materials compared to the certified and reported values by the Community Bureau of Reference BCR. The detection limit in the extracts was established as 1 μg L^{-1}.

Table 1
Selected soil physical and chemical properties.

pH	CEC (cmol(+) kg^{-1})	EC (dS m^{-1})	Clay:Silt:Sand (%)	OC (%)	Ni concentration (mg kg^{-1})	Origin
6.4	12	0.12	5:8:87	3.0	18.6 ± 4.3	Eiken, Switzerland

Samples of the control and Ni-spiked soils were ground using a Retsch RS1 grinder with a tungsten carbide ball and ring, pressed into pellets and analysed by X-ray fluorescence (X-Lab 2000, Spectro, Kleve, Germany) for major elements, including Ca, Mg, Fe, and Ni. The analytical quality of the XRF measurements was routinely controlled by use of a certified standard sample (D133, MCACAL).

2.2. LA-ICP-MS analysis

The LA-ICP-MS system consisted of a 193 nm neodymium-doped yttrium aluminum garnet laser (New Wave Research, Huntingdon, UK) for sampling and a quadrupole inductively coupled plasma mass spectrometer (ICP-Q-MS, ELAN 6100 DRC-e, PerkinElmer, Ontario, Canada), for analysing the ablated sample. The ablation cell was coupled via a 50-cm PFA-tubing to the ICP-torch. Argon was used as carrier gas

The surfaces of the cross-sections were pre-ablated to eliminate possible contamination caused by the cutting process. For the pre-ablation, we used line scan mode (ablating along a line) with a laser beam diameter of 120 μm, a laser fluence of 6 J cm^{-2} and a scan speed of 20 μm s^{-1} ablating a depth of about 5 μm. After pre-ablation, the samples were scanned using a laser fluence of 15 J cm^{-2} at a frequency of 10 Hz, a laser beam diameter of 75 μm and a scan speed of 5 μm s^{-1}. The frequency of the laser was kept at 10 Hz. This leads to a spatial resolution of about 75 μm × 10 μm. The sampling depth was about 10 μm and varied with the density of the tissue. This variation was overcome by using a homogenously occurring element (e.g. carbon) as internal normalization standard leading thus to a gravimetrical measurement quantity in μg g^{-1} instead of a volumetric quantity in μg cm^{-3}. The resulting inhomogeneities of the ablation conditions due to tissue density variation are considered in the uncertainty calculation. Depending on the diameter of the root cross-section, each cross-section was ablated five or six times along parallel patterns to cover the entire root cross-section area.

An element with a known concentration that is homogeneously distributed in reference material and the samples is used for internal normalization of the signal to correct for any differences in ablation rates (Longerich et al., 1996, 1997). Thus, a response factor (Cromwell and Arrowsmith, 1995; Motelica-Hieno and Donard, 2001; Resano et al., 2005) for each analyte relative to the internal standard in the reference material can be calculated. The response factor reflects sensitivity differences between the analyte, *E*, and the element used as internal standard. Assuming that the response factor is the same for reference material and the sample, the concentration of an element *E* in the sample can be calculated as follows:

$$C_{\mathrm{Sam}}(E) = \left(\frac{I_{E\mathrm{Sam}} C_{E\mathrm{Ref}}}{I_{\mathrm{ISSam}} C_{\mathrm{ISRef}}}\right) C_{\mathrm{ISSam}} \left(\frac{I_{\mathrm{ISRef}}}{I_{E\mathrm{Ref}}}\right), \quad (1)$$

where $C_{\mathrm{IS\,Sam}}$ is the independently measured concentration of the internal standard in the sample, $C_{E\,\mathrm{Ref}}/C_{\mathrm{IS\,Ref}}$ is the ratio of the concentrations of analyte *E* and internal standard IS in the certified reference material, and $I_{E\,\mathrm{Sam}}/I_{\mathrm{IS\,Sam}}$ and $I_{\mathrm{IS\,Ref}}/I_{E\,\mathrm{Ref}}$ are the intensity ratios measured in sample and reference material, respectively.

We used the response factor given in the Elan DRC-e software to calculate the concentrations in the samples. The concentration of analyte, *E*, is calculated using the relative sensitivity coefficient (RSC) from the ELAN DRC-e ICP-MS:

$$C_{\mathrm{Sam}}(E) = \frac{(I_{E\mathrm{Sam}}/I_{\mathrm{ISSam}})C_{\mathrm{ISSam}}}{RSC_{\mathrm{ICP\text{-}MS}}} \quad (2)$$

Multiple isotopes per element were measured if accessible for each element to monitor possible interferences. Generally, we used carbon as the internal standard since it is the major element present in the root matrix (Prohaska et al., 1998). Nonetheless, the use of carbon showed limitations in the used setup which were: (i) the relatively high background signal of carbon and (ii) the low sensitivity of C of the quadrupole ICP-MS. Major reason for the latter is the fact that the Elan does not apply an extraction voltage to the generated ions. Thus, we observed a significant diffusion of the light carbon ions and a signal to noise ratio, which is not satisfactory for small signals (i.e., resulting from small spot diameters). Nonetheless, we observed at larger spot sizes (<100 μm) that the signals at mass 42 and 44 are evenly distributed along with the C signal with a relative standard deviation (RSD) across the single root surfaces of less than 8%. Both masses refer to Ca and since the ratios of these masses correspond to the natural abundances, interferences can be excluded. Therefore, we used finally ^{44}Ca as internal standard for the analysis of Ni, Mg, and Fe. The uncertainty of the relative variation of the elemental content (semi-quantitative data) is about 10% whereas the quantitative data has an uncertainty of about 25%. Uncertainties were calculated according to EURACHEM using a dedicated software (Gum Workbench Pro, Metrodata, Danish Technological institute, Danmark). Total Ca of the roots was determined using ICP-OES.

2.3. DMG staining and image processing

The risk of artifacts from Ni redistribution in the course of the staining procedure depends on the solvent and the time between DMG application and imaging. We tested various solvents that previous studies have proposed, on plant samples that were prepared using similar method. Based on these preliminary tests, we selected a DMG solution containing 1 g DMG and 0.18 g KOH dissolved in 100 ml of 0.025 M $Na_2B_4O_7$, 10 H_2O solution (Merck, Darmstadt, Germany). This solution gave the best staining quality while preserving plant structure (Gramlich et al., 2007). Comparing various sample preparation methods and immersion times, the procedure that gave the best results was as follows: A droplet of 30 μl of the DMG solution was applied to freshly cut root cross sections of 150 μm thickness. Immediately after adding the droplet, the cross section was imaged using light microscopy and photographed using a digital camera (Canon Power Shot A640).

Principal component analysis was used to separate the signal originating from the dye (DMG-Ni stain) from the rest of the image in order to obtain a qualitative measure of DMG-Ni stain in the root cross-section. Inspections of collocation histograms for the color channel combinations Red–Green (RG), Red–Blue (RB), and Green–Blue (GB) showed that the RG combination was the best suited for this separation. For the principal component analysis, we followed the procedure explained by Jain (1989) and known as Karhunen-Loewe transformation. The procedure uses the eigenvector matrix derived from the covariance matrix of the two color channels as a linear transformation matrix for the two channels to obtain the independent basis images. The basis image corresponding to the greater eigenvalue contains the information of the DMG-Ni stain.

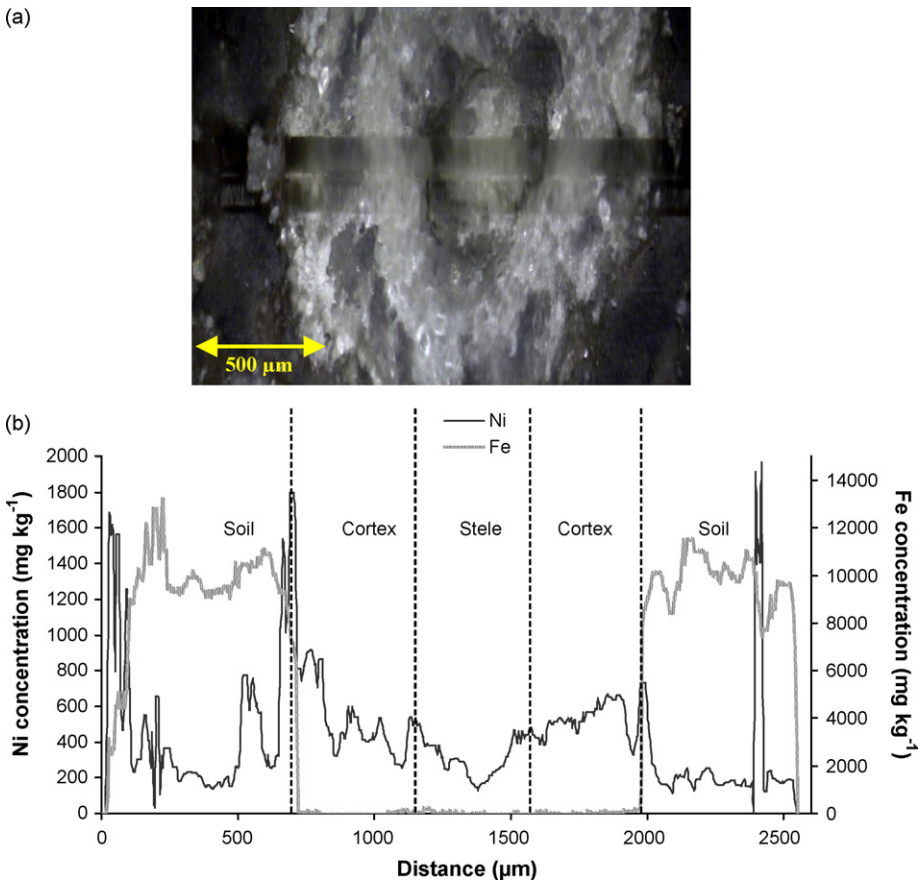

Fig. 1. Laser image of a cross-section through a *B. coddii* root and surrounding soil (a) and Ni and Fe concentration profiles along a scan-line across the cross-section (b). The soil was spiked with 125 mg kg^{-1} Ni.

Image analysis was carried out using MATLAB (Matlab, 2007). All the images were slightly smoothed using a median filter of 3×3. All statistical comparisons were done using analysis of variance ANOVA, while the confidence coefficient was set at 0.05.

3. Results

3.1. Analysis using LA-ICP-MS scan-lines

Fig. 1a shows a laser image with two adjacent laser scan-lines passing through the cross-section of a *B. coddii* root grown in the soil containing 125 mg kg^{-1} Ni. The cortex and the stele of the root are clearly visible. The Ni concentration along one of the two laser lines is shown in Fig. 1b. The nickel concentration varied from 100 to 1800 mg kg^{-1} in the soil adjacent to the root due to the heterogeneous distribution of soil particles and pores. The average concentration was higher inside the roots and less variable than in the soil. We used the Fe: Ni ratio to locate the epidermis. Inside the root, the iron concentration dropped to a value below 100 mg kg^{-1}, while the Ni concentration stayed above the average value of the soil Ni concentration. In addition, we observed an increase of the Fe concentration near the epidermis before it started to decline inside the root. Similar Fe peaks were monitored adjacent to the epidermis of the roots that had been washed in deionised water before being embedded in resin. The iron can be attributed to residual soil micro particulates attached to the surface. Some soil particles may not be removable because of the roughness of the root surface and micro particles may remain trapped in root fractures while growing (Tinker and Nye, 2000). The minimum Ni concentration within the root was measured in the stele in the centre of the root. The Ni concentration averaged around 500 mg kg^{-1} in the cortex and less than 300 mg kg^{-1} in the stele.

3.2. Analysis of DMG-stained root cross-sections

Fig. 2 shows a cross-section of a root grown in the soil containing 125 mg kg^{-1} Ni, with almost the same diameter as the root in Fig. 1. The root in Fig. 2a was freshly cut and stained with DMG. The red area shows where the Ni-DMG complexes were located in the root. Fig. 2a shows that the cortex was stained more intensively than the stele. Within the cortex, the red intensity was higher in the apoplastic space within and around the cell walls than in the cytoplasm. Transformation of the image by Karhunen-Loewe transformation resulted in Fig. 2b. The red intensity in this image qualitatively corresponds to the intensity of Ni-DMG complex. The overall Ni profiles were similar in both Fig. 2c and Fig. 1c. In other words, the average Ni concentration and red intensity were higher in the cortex than in the stele. The stele had the lowest Ni concentration and red intensity while the epidermis had the highest Ni concentration and red intensity. However, there was a sharp contrast between the red intensity of cortex and stele in Fig. 2c. Conversely, the Ni concentration profile in laser cross-section (Fig. 1c) was less homogeneous and the difference in average Ni concentration between the cortex and the stele was not as sharp as in Fig. 2 c.

3.3. Two-dimensional map of Ni in root cross-section

Seven parallel laser scan-lines were recorded from a root cross-section of the 125 mg kg^{-1} Ni treatment to cover the entire root cross-section area. Fig. 3 shows an example of a 2-dimensional

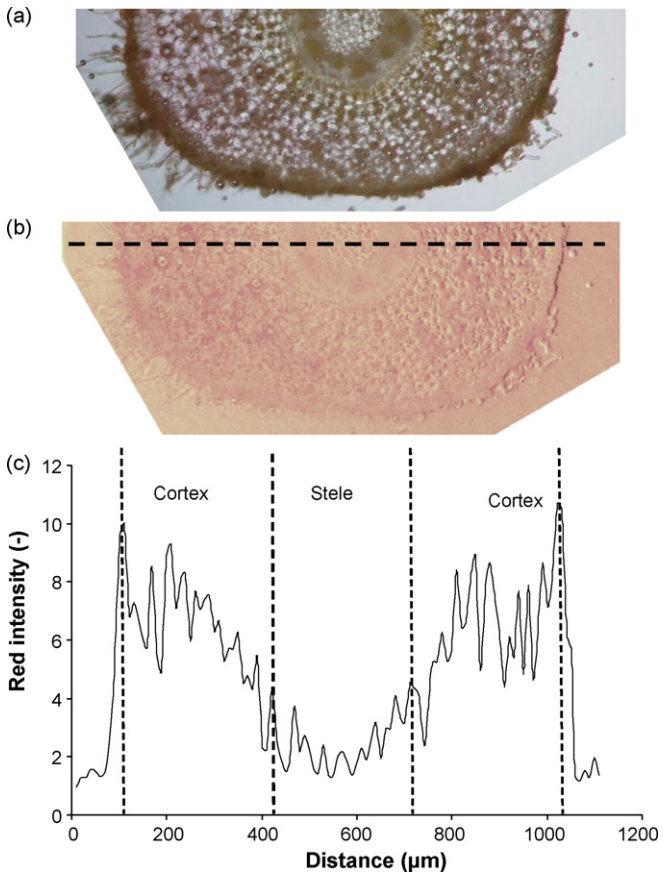

Fig. 2. Microscopic image of a root cross-section of Ni-hyperaccumulator plant *B. coddii* grown in the Ni-spiked soil and stained with DMG solution (a), the same image after processing using Karhunen-Loewe transformation to separate the dye signal from the rest of the image (b) and the resulting red intensity profile along the root cross-section (c). The red intensity is a qualitative indicator of the DMG-Ni complex.

map of the Ni concentration of the root cross-section calculated from these scan-lines. The nickel concentrations varied from 100–500 mg kg^{-1}. The highest concentrations of Ni occurred in small spots that were distributed heterogeneously within the cortex. The stele showed a more homogenous distribution of Ni pattern and had lower concentration of Ni than the cortex. This observation was reproducible throughout five measured root cross sections.

Likewise, six laser scan-lines were recorded from a cross-section of a root grown in the control soil. The resulting 2-D map of Ni concentration is shown in Fig. 4. Unlike the roots in the spiked soil, the highest concentration of Ni appeared in the stele. The average Ni concentration was around 50 mg kg^{-1} compared to 22 mg kg^{-1} in the cortex. Similar trend was observed for all five replicates.

3.4. Comparing LA-ICP-MS and DMG staining results

Fig. 5 shows a comparison between the Ni concentrations measured by means of LA-ICP-MS and the red intensities of the DMG-staining for both control and Ni-treated roots. Five replicates for each treatment were used to calculate the average and standard deviation of the Ni concentration and red intensity of various tissues of the roots. The cortex was divided equally into the outer and inner cortex, while the overall average of the stele was calculated. The background refers to either the resin around the roots in laser ablation experiment or an open area without any sample in DMG-staining experiment. Root diameters ranged from 1 to 1.5 mm.

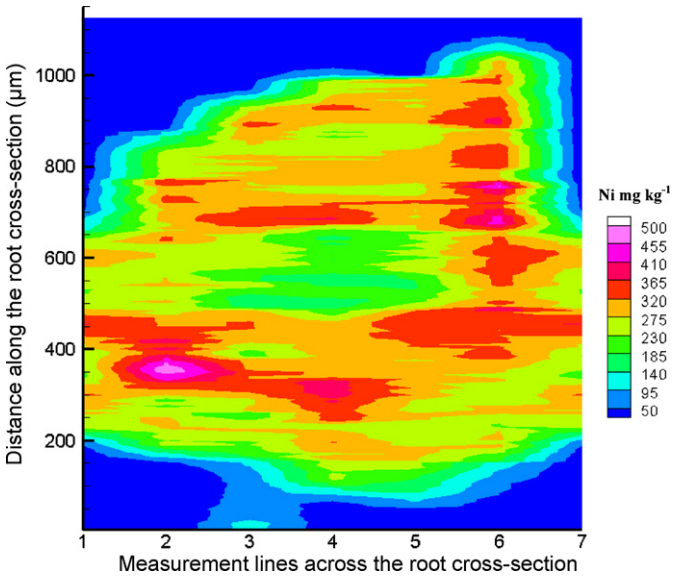

Fig. 3. Semi-quantitative Ni map of the root cross-section of Ni-hyperaccumulator plant *B. coddii* grown on the soil spiked with 125 mg kg^{-1} Ni. The image was slightly smoothed to reduce the noise.

LA-ICP-MS measurements of roots of the Ni-spiked treatment (Fig. 5a) showed no significant difference (based on analysis of variance, ANOVA) between the outer and inner cortex (373 ± 63 and 375 ± 70 mg kg^{-1}, respectively), while the Ni concentrations of the stele was significantly lower (210 ± 48 mg kg^{-1}). In the DMG-stained roots of the same treatment (Fig. 5b), however, the red intensity decreased from the outer to the inner cortex. While there was no significant difference between the inner cortex and the stele, they both had significant lower intensities than the outer cortex. Again, the stele had higher intensities than the background.

In contrast to the Ni-spiked treatment, the roots grown in the control soil (Fig. 5c), had higher Ni concentrations in the stele (32 ± 7 mg kg^{-1}) than in the cortex, while there was no significant difference between the outer and inner cortex (19 ± 5 and 17 ± 3 mg kg^{-1}, respectively). There was no significant difference between the cortex and the stele for the red intensity in the DMG-stained roots from the control soil. However, the control samples had significantly higher red intensities than the back-

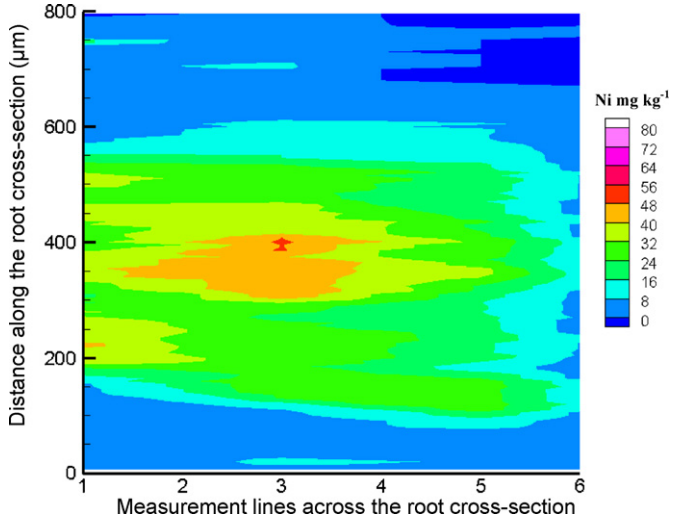

Fig. 4. Semi-quantitative Ni map of the root cross-section of Ni-hyperaccumulator plant *B. coddii* grown on the control soil. The image was slightly smoothed to reduce the noise.

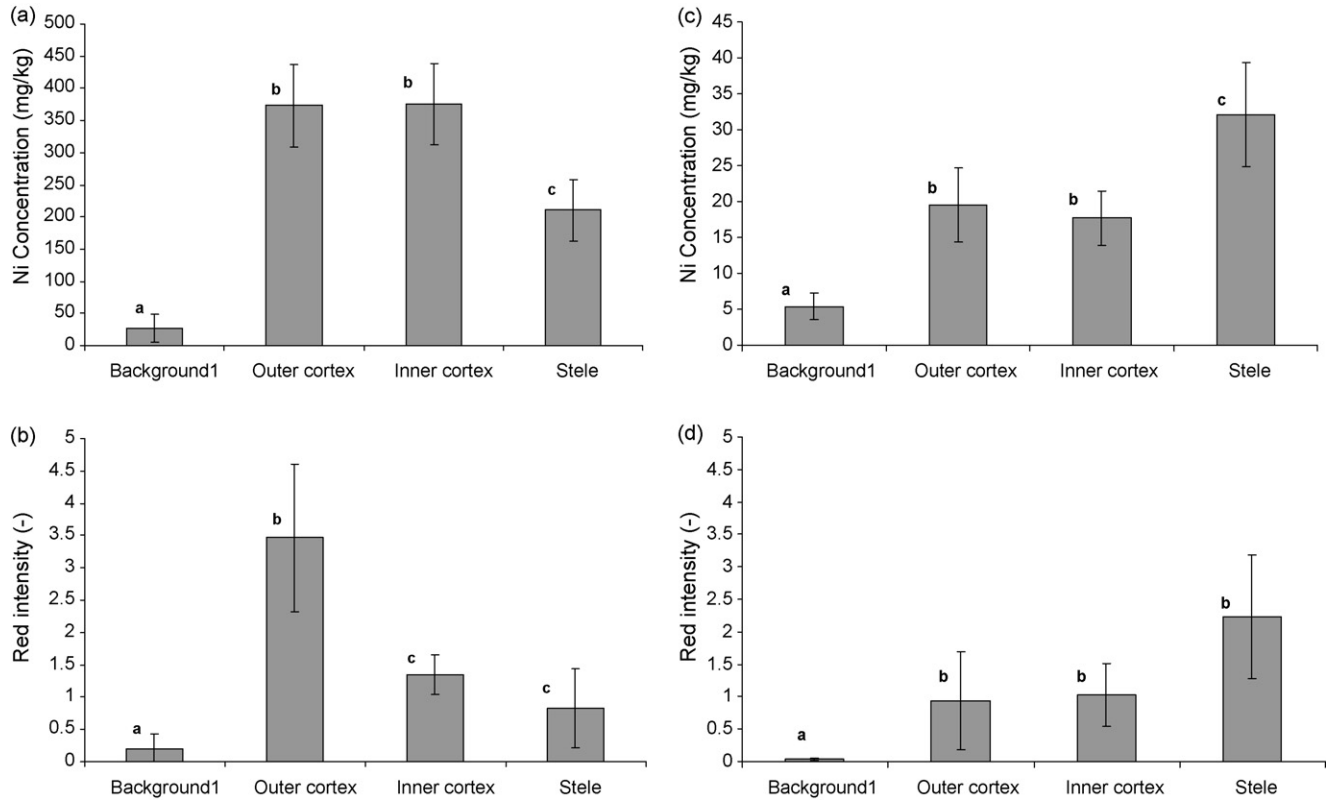

Fig. 5. Average Ni concentrations (measured using LA-ICP-MS) in different root tissues of the Ni-hyperaccumulator *B. coddii* grown on the soil spiked with 125 mg kg^{-1} Ni (a) and unspiked soil (c) and the qualitative red intensity of DMG staining method for the corresponding tissues in spiked soil (b) and unspiked soil (d). The error bars represent standard deviations; bars with different letters were significantly different at the 0.05 level.

ground (Fig. 5d). A higher Ni background was measured in the resin adjacent to the roots grown in the Ni-spiked soil compared to the control soil (5 ± 2 and 27 ± 22 mg kg^{-1}, respectively). This effect can be explained by Ni in the soil particles attached to the roots.

3.5. Total Ni content in roots measured by LA-ICP-MS, ICP-OES and XRF

Table 2 summarizes the results of the elemental analysis of the soil and roots using XRF, ICP-OES and LA-ICP-MS. The values obtained by LA-ICP-MS were weighted by the area contribution of each tissue to the root cross-section area. All results show high variation and thus a large standard deviation. This is due to heterogeneity of the sample material. There was no significant difference (ANOVA at 0.05 level) between the Ni values for roots grown in the control soil measured by the three different techniques. However the results for ICP-OES measurements were extremely variable (29.2 ± 27). This can be explained mainly by unsatisfactory separation of soil particles from the roots prior to digestion and is in accordance with our observation of the Ni background in the resin adjacent to the root surface. Similar to the control soil, there was no significant difference between the LA-ICP-MS and the ICP-OES values for the Ni-spiked root (ANOVA at 0.05 level). LA-ICP-MS gave significantly smaller values for Fe compared to ICP-OES. This may have been caused again by incomplete separation of soil particles from the roots prior to digestion and subsequent ICP-OES analysis, as well. The Mg concentration in the roots was in good agreement for both ICP-OES and LA-ICP-MS and the results overlapped within the standard deviation.

Table 2
Elemental concentrations (mg kg^{-1}) of the roots and soil using various techniques. Values in parenthesis show standard deviations from the mean.

			XRF	ICP-OES	LA-ICP-MS*
Ni	Control	Soil	18.6 (4.3)	**n.q.	n.q.
		Root	n.q.	***[a] 29.2 (27)	[a] 22.2 (5.4)
	Ni-spiked	Soil	113.8 (29)	n.q.	n.q.
		Root	n.q.	[a] 465.1 (70.1)	[a] 333.2 (60)
Fe	Control	Soil	14180 (548)	n.q.	n.q.
		Root	n.q.	[a] 80.3 (67)	[a] 24.2 (44)
	Ni-spiked	Soil	14330 (320)	n.q.	n.q.
		Root	n.q.	[a] 143.6 (38)	[b] 32.3 (53.7)
Mg	Control	Soil	4260 (170)	n.q.	n.q.
		Root	n.q.	[a] 1954.5 (841)	[a] 2243 (393)
	Ni-spiked	Soil	4560 (216)	n.q.	n.q.
		Root	n.q.	[a] 2115.3 (1121)	[a] 2940 (270)

*Averages were calculated based on the area contribution of each tissue for roots. **n.q.: not quantified. ***In each row, different letters represent significance at 0.05 level.

4. Discussion

We obtained a similar pattern of Ni distribution in the root tissue using two independent techniques. This indicates that either redistribution did not greatly affect our results, or the redistribution was the same for both methods, which is unlikely. Bhatia et al. (2004) reported that DMG application lead to Ni redistribution inside the plant tissue. The staining procedure they used involved soaking the plant tissue in DMG solution (1% solution in 95% ethanol) over night. Ethanol is very damaging to the tissue and increases the risk of Ni redistribution especially if applied for a rather long time. Our procedure included no ethanol and the time given to the DMG solution to react with Ni in the tissue was less than half a minute before the image was taken. Such a short exposure time reduces both the downward penetration and lateral redistribution of DMG-Ni complex in the tissue. Although such redistributions might be significant at the cellular and sub-cellular level, but it is unlikely to be considerable at the tissue level.

DMG staining provided qualitative data on the distribution of Ni in the root cross-sections. DMG might not be able to stain some tightly bound (or more likely) occluded Ni in some tissues; nevertheless, it represents the biologically active Ni. DMG strongly bonds to Ni. Its log stability constant is reported to be 17.2 which is comparable to strong complexing agents such as EDTA with log stability constant of 18.4 (Saito and Moffett, 2001). Therefore, it could be used to differentiate between different types of Ni in biological tissues.

LA-ICP-MS method provided semi-quantitative data on the distribution of metals within the root cross-sections of *B. coddii*. The spatial resolution of the data was sufficient for root studies at tissue level. The laser scan-lines gave a resolution of 75 μm $\times$ 10 μm. The spatial resolution was fine in the direction of the scan-lines, but coarse in the perpendicular direction because of the scan width. The width was selected in order to receive sufficient signal intensities. Nonetheless, narrower scan lines can be a significant improvement in lateral resolution but this also means the need for combination with ICP-MS instruments with higher sensitivity. Moreover, matrix artifacts due to resin embedding could challenge the accuracy and precision of the technique at resolutions finer than tissue level. Staining the root cross-section with DMG revealed a comparable pattern of Ni distribution in the root cross-sections (compare Figs. 1 and 2). Although the DMG-staining had a higher spatial resolution in all directions than LA-ICP-MS, it provided only qualitative information.

Both techniques showed that the Ni concentration was higher in the cortex of roots grown in the Ni-spiked soil than in the stele. The DMG-staining experiment showed that the concentrations of Ni decreased from the outer cortex towards the inner cortex and the stele. Similar result was reported by Mesjasz-Przybylowicz et al. (2007) in the roots of another Ni hyperaccumulator plant, *Senecio coronatur*. The DMG-staining experiment revealed that the Ni was more concentrated in the apoplastic area than in the cytoplasm. As supported by other investigations (Gramlich et al., 2007; Redjala et al., 2009), this proves that apoplastic pathway is the main means of Ni transport in the cortex. The role of the endodermis is to provide a barrier to the apoplastic pathway (Marschner, 1995). This affects the passage of all solutes including Ni. Our results are consistent with what is known about the endodermis. This information could not be obtained by LA-ICP-MS because of the spatial resolution we chose and the physical shrinkage of the tissue that resulted from sample preparation.

Two-dimensional map of Ni concentration obtained by LA-ICP-MS method showed small spots of high Ni concentration in the root cross-sections from the Ni-spiked soil. These spots were randomly distributed in the cortex. We hypothesize that they are either caused by co-precipitation of Ni with phosphate in the apoplast as has been reported for other hyperaccumulator plants (Zhao et al., 2000), or they are some artifacts created during sample fixation process.

As has been shown in previous studies (Puschenreiter et al., 2005; Moradi et al., 2010), abundant presence of Ni in the rhizosphere, mass flow of water, and free movement in the apoplastic pathway can explain high concentration of Ni in the cortex. Considering the Ni content of ultramafic soils, where *B. coddii* is native (Morrey et al., 1992), this is likely to be the case in its native environment. On the other hand, Ni concentration was found to be higher in the stele than in the cortex of the roots in control soil with low Ni concentration. The difference in Ni concentration of cortex and stele indicates active uptake or at least a selection mechanism for Ni ions in the latter case, since the uptake occurred against the concentration gradient. Therefore, nickel needs to pass through ion pumps or selective channels, which requires metabolic energy.

5. Conclusions

The semi-quantitative two-dimensional Ni distribution pattern in the root cross-sections of the Ni hyperaccumulator plant *B. coddii* obtained using LA-ICP-MS method were supported qualitatively by DMG-staining technique showing a greater concentration of Ni in the cortex of the Ni-spiked roots than in the stele, while the opposite pattern was observed for the control roots. Obtaining similar Ni distribution patterns using two independent methods (including sample preparation) indicates that possible artifacts due to redistribution of Ni within the root tissue during sample preparation were inconsequent. DMG-staining proved to be a fast and low-cost method for qualitative studying of Ni distribution in plant tissues. The result underlines that direct analysis of roots and rhizosphere areas show a great potential in gaining a better understanding of the Ni concentration gradient in the rhizosphere of *B. coddii* to unravel more information regarding uptake of Ni and its distribution inside the roots.

Acknowledgements

We would like to thank Jakob Frommer for his technical support for embedding and preparing the root samples. This study was funded by the Swiss National Science Foundation and the Austrian Science Fund (FWF–START project 267 N11)

References

Angle, J.S., Chaney, R.L., Baker, A.J.M., Li, Y., Reeves, R., Volk, V., Roseberg, R., Brewer, E., Burke, S., Nelkin, J., 2001. Developing commercial phytoextraction technologies: practical considerations. South African Journal of Science 97, 619–623.

Becker, J.S., Dietrich, R.C., Matusch, A., Pozebon, D., Dressier, V.L., 2008. Quantitative images of metals in plant tissues measured by laser ablation inductively coupled plasma mass spectrometry. Spectrochimica Acta Part B-Atomic Spectroscopy 63, 1248–1252.

Becker, J.S., Zoriy, M.V., Pickhardt, C., Palomero-Gallagher, N., Zilles, K., 2005. Imaging of copper, zinc, and other elements in thin section of human brain samples (Hippocampus) by laser ablation inductively coupled plasma mass spectrometry. Analytical Chemistry 77, 3208–3216.

Berazain, R., de la Fuente, V., Rufo, L., Rodriguez, N., Amils, R., Diez-Garretas, B., Sanchez-Mata, D., Asensi, A., 2007. Nickel localization in tissues of different hyperaccumulator species of *Euphorbiaceae* from ultramafic areas of Cuba. Plant and Soil 293, 99–106.

Bhatia, N.P., Walsh, K.B., Orlic, I., Siegele, R., Ashwath, N., Baker, A.J.M., 2004. Studies on spatial distribution of nickel in leaves and stems of the metal hyperaccumulator *Stackhousia tryonii* using nuclear microprobe (micro-PIXE) and EDXS techniques. Functional Plant Biology 31, 1061–1074.

Broadhurst, C.L., Chaney, R.L., Angle, J.S., Erbe, E.F., Maugel, T.K., 2004. Nickel localization and response to increasing Ni soil levels in leaves of the Ni hyperaccumulator Alyssum murale. Plant and Soil 265, 225–242.

Brooks, R.R., Chambers, M.F., Nicks, L.J., Robinson, B.H., 1998. Phytomining. Trends in Plant Science 3, 359–362.

Budka, D., Mesjasz-Przybylowicz, J., Tylko, G., Przybylowlicz, W.J., 2005. Freeze-substitution methods for Ni localization and quantitative analysis in *Berkheya coddii* leaves by means of PIXE. Nuclear Instruments & Methods in Physics

Research Section B-Beam Interactions with Materials and Atoms 231, 338–344.
Cromwell, E.F., Arrowsmith, P., 1995. Semiquantitative analysis with laser-ablation inductively-coupled plasma-mass spectrometry. Analytical Chemistry 67, 131–138.
de la Fuente, V., Rodriguez, N., Diez-Garretas, B., Rufo, L., Asensi, A., Amils, R., 2007. Nickel distribution in the hyperaccumulator *Alyssum serpyllifolium* Desf. spp. from the Iberian Peninsula. Plant Biosystems 141, 170–180.
Dessureault-Rompre, J., Nowack, B., Schulin, R., Luster, J., 2006. Modified micro suction cup/rhizobox approach for the in-situ detection of organic acids in rhizosphere soil solution. Plant and Soil 286, 99–107.
Eeckhaoudt, S., Vandeputte, D., Vanpraag, H., Vangrieken, R., Jacob, W., 1992. Laser microprobe mass analysis (LAMMA) of aluminum and lead in fine roots and their ectomycorrhizal mantles of Norway spruce. Tree Physiology 10, 209–215.
Fahrni, C.J., 2007. Biological applications of X-ray fluorescence microscopy: exploring the subcellular topography and speciation of transition metals. Current Opinion in Chemical Biology 11, 121–127.
Gramlich, A.M., Moradi, A.B., Robinson, B.H., Kaesner, A., Schulin, R., 2007. The semi-quantitative distribution of Ni in plant tissues using DMG staining and image processing. Submitted to Environmental and Experimental Botany.
Hall, J.L., 2002. Cellular mechanisms for heavy metal detoxification and tolerance. Journal of Experimental Botany 53, 1–11.
Hattendorf, B., Latkoczy, C., Gunther, D., 2003. Laser ablation-ICPMS. Analytical Chemistry 75, 341A–347A.
Heath, S.M., Southworth, D., Dallura, J.A., 1997. Localization of nickel in epidermal subsidiary cells of leaves of Thlaspi montanum var siskiyouense (Brassicaceae) using energy-dispersive x-ray microanalysis. International Journal of Plant Sciences 158, 184–188.
Hoagland, D.R., Arnon, D.I., 1938. The water culture method for growing plants without soil. California: Agricultural Experiment Station 347, 1–39.
Jain, A., 1989. Fundamentals of digital image processing. Prentice Hall, Englewood Cliffs, NJ.
Kaiser, J., Galiová, M., Novotný, J., Červenka, R., Reale, L., Novotný, J., Liška, M., Samek, O., Kanický, V., Hrdlička, A., Stejskal, K., Adam, V., Kizek, R., 2008. Mapping of lead, magnesium and copper accumulation in plant tissues by laser-induced breakdown spectroscopy and laser-ablation inductively coupled plasma mass spectrometry. Spectrochimica Acta Part B, Atomic Spectroscopy, Amsterdam, Elsevier, The Nederlands. ISSN 0584-8547, 2009, vol. 64, no. 1, pp. 67–73.
Kindness, A., Sekaran, C.N., Feldmann, J., 2003. Two-dimensional mapping of copper and zinc in liver sections by laser ablation-inductively coupled plasma mass spectrometry. Clinical Chemistry 49, 1916–1923.
Kramer, U., CotterHowells, J.D., Charnock, J.M., Baker, A.J.M., Smith, J.A.C., 1996. Free histidine as a metal chelator in plants that accumulate nickel. Nature 379, 635–638.
Kylander, M.E., Weiss, D.J., Jeffries, T.E., Kober, B., Dolgopolova, A., Garcia-Sanchez, R., Coles, B.J., 2007. A rapid and reliable method for Pb isotopic analysis of peat and lichens by laser ablation-quadrupole-inductively coupled plasma-mass spectrometry for biomonitoring and sample screening. Analytica Chimica Acta 582, 116–124.
Li, Y.M., Chaney, R., Brewer, E., Roseberg, R., Angle, J.S., Baker, A., Reeves, R., Nelkin, J., 2003. Development of a technology for commercial phytoextraction of nickel: economic and technical considerations. Plant and Soil 249, 107–115.
Lobinski, R., Moulin, C., Ortega, R., 2006. Imaging and speciation of trace elements in biological environment. Biochimie 88, 1591–1604.
Longerich, H.P., Jackson, S.E., Gunther, D., 1996. Laser ablation inductively coupled plasma mass spectrometric transient signal data acquisition and analyte concentration calculation. Journal of Analytical Atomic Spectrometry 11, 899–904.
Longerich, H.P., Jackson, S.E., Gunther, D., 1997. Laser ablation inductively coupled plasma mass spectrometric transient signal data acquisition and analyte concentration calculation (vol 11, pg 899, 1996). Journal of Analytical Atomic Spectrometry 12, 391–1391.
Ma, J.F., Ueno, D., Zhao, F.J., McGrath, S.P., 2005. Subcellular localisation of Cd and Zn in the leaves of a Cd-hyperaccumulating ecotype of Thlaspi caerulescens. Planta 220, 731–736.
Marschner, H., 1995. Mineral Nutrition of Higher Plants. Academic Press, London.
Martin, R.R., Naftel, S.J., Macfie, S., Skinner, W., Courchesne, F., Seguin, V., 2004. Time of flight secondary ion mass spectrometry studies of the distribution of metals between the soil, rhizosphere and roots of *Populus tremuloides* Minchx growing in forest soil. Chemosphere 54, 1121–1125.
Matlab, 2007. The Math Works, Inc., Natick, MA 01760-2098, United States.
McNear, D.H., Peltier, E., Everhart, J., Chaney, R.L., Sutton, S., Newville, M., Rivers, M., Sparks, D.L., 2005. Application of quantitative fluorescence and absorption-edge computed microtomography to image metal compartmentalization in Alyssum murale. Environmental Science & Technology 39, 2210–2218.
Mesjasz-Przybylowicz, J., Barnabas, A., Przybylowicz, W., 2007. Comparison of cytology and distribution of nickel in roots of Ni-hyperaccumulating and non-hyperaccumulating genotypes of *Senecio coronatus*. Plant and Soil 293, 61–78.
Mesjasz-Przybylowicz, J., Przybylowicz, W.J., Pineda, C.A., 2001. Nuclear microprobe studies of elemental distribution in apical leaves of the Ni hyperaccumulator *Berkheya coddii*. South African Journal of Science 97, 591–593.
Metzner, R., Schneider, H.U., Breuer, U., Schroeder, W.H., 2008. Imaging nutrient distributions in plant tissue using time-of-flight secondary ion mass spectrometry and scanning electron microscopy. Plant Physiology 147, 1774–1787.
Mizuno, N., Nosaka, S., Mizuno, T., Horie, K., Obata, H., 2003. Distribution of Ni and Zn in the leaves of Thlaspi japonicum growing on ultramafic soil. Soil Science and Plant Nutrition 49, 93–97.
Moradi, A.B., Conesa, H.M., Robinson, B.H., Lehmann, E., Kaestner, A., Schulin, R., 2009. Root responses to soil Ni heterogeneity in a hyperaccumulator and a non-accumulator species. Environmental Pollution 157, 2189–2196.
Moradi, A.B., Oswald, S.E., Nordmeyer-Massner, J.A., Pruessmann, K.P., Robinson, B.H., Schulin, R., 2010. Analysis of nickel concentration profiles around the roots of the hyperaccumulator plant *Berkheya coddii* using MRI and numerical simulations. Plant and Soil 328, 291–302. Published online, doi:10.1007/s11104-009-0109-8.
Morrey, D.R., Balkwill, K., Balkwill, M.J., Williamson, S., 1992. A review of some studies of the serpentine flora of Southern Africa. In: Baker, A.J.M., Procter, J., Reeves, R.D. (Eds.), The Vegetation of Ultramafic (Serpentine) Soils. Intercept, Andover, pp. 147–158.
Motelica-Hieno, M., Donard, O.F.X., 2001. Comparison of UV and IR laser ablation ICP-MS on silicate reference materials and implementation of normalisation factors for quantitative measurements. Geostandards Newsletter-the Journal of Geostandards and Geoanalysis 25, 345–359.
Pickhardt, C., Dietze, H.J., Becker, J.S., 2005. Laser ablation inductively coupled plasma mass spectrometry for direct isotope ratio measurements on solid samples. International Journal of Mass Spectrometry 242, 273–280.
Prohaska, T., Stadlbauer, C., Wimmer, R., Stingeder, G., Latkoczy, C., Hoffmann, E., Stephanowitz, H., 1998. Investigation of element variability in tree rings of young Norway spruce by laser-ablation-ICPMS. Science of the Total Environment 219, 29–39.
Przybylowicz, W.J., Mesjasz-Przybylowicz, J., Pineda, C.A., Churms, C.L., Ryan, C.G., Prozesky, V.M., Frei, R., Slabbert, J.P., Padayachee, J., Reimold, W.U., 2001. Elemental mapping using proton-induced X-rays. X-Ray Spectrometry 30, 156–163.
Puschenreiter, M., Schnepf, A., Millan, I.M., Fitz, W.J., Horak, O., Klepp, J., Schrefl, T., Lombi, E., Wenzel, W.W., 2005. Changes of Ni biogeochemistry in the rhizosphere of the hyperaccumulator *Thlaspi goesingense*. Plant and Soil 271, 205–218.
Redjala, T., Sterckeman, T., Skiker, S., Echevarria, G., 2009. Contribution of apoplast and symplast to short term nickel uptake by maize and Leptoplax emarginata roots. Environmental and Experimental Botany 68, 99–106.
Resano, M., Perez-Arantegui, J., Garcia-Ruiz, E., Vanhaecke, F., 2005. Laser ablation-inductively coupled plasma mass spectrometry for the fast and direct characterization of antique glazed ceramics. Journal of Analytical Atomic Spectrometry 20, 508–514.
Robinson, B.H., Brooks, R.R., Howes, A.W., Kirkman, J.H., Gregg, P.E.H., 1997. The potential of the high-biomass nickel hyperaccumulator *Berkheya coddii* for phytoremediation and phytomining. Journal of Geochemical Exploration 60, 115–126.
Robinson, B.H., Lombi, E., Zhao, F.J., McGrath, S.P., 2003. Uptake and distribution of nickel and other metals in the hyperaccumulator *Berkheya coddii*. New Phytologist 158, 279–285.
Russo, R.E., Mao, X.L., Liu, H.C., Gonzalez, J., Mao, S.S., 2002. Laser ablation in analytical chemistry – a review. Talanta 57, 425–451.
Saito, M.A., Moffett, J.W., 2001. Complexation of cobalt by natural organic ligands in the Sargasso Sea as determined by a new high-sensitivity electrochemical cobalt speciation method suitable for open ocean work. Marine Chemistry 75, 49–68.
Shi, J.Y., Gras, M.A., Silk, W.K., 2009. Laser ablation ICP-MS reveals patterns of copper differing from zinc in growth zones of cucumber roots. Planta 229, 945–954.
Tappero, R., Peltier, E., Grafe, M., Heidel, K., Ginder-Vogel, M., Livi, K.J.T., Rivers, M.L., Marcus, M.A., Chaney, R.L., Sparks, D.L., 2007. Hyperaccumulator Alyssum murale relies on a different metal storage mechanism for cobalt than for nickel. New Phytologist 175, 641–654.
Tinker, P.B., Nye, P.H., 2000. Solute movement in the rhizosphere. Oxford University Press, New York.
Ulrich, A., Barrelet, T., Krahenbuhl, U., 2007. Spatially resolved plant physiological analysis using LA-HR-ICP-MS. Chimia 61, 111–1111.
Zhao, F.J., Lombi, E., Breedon, T., McGrath, S.P., 2000. Zinc hyperaccumulation and cellular distribution in *Arabidopsis halleri*. Plant Cell and Environment 23, 507–514.